ISSN: 2155-9546
Journal of Aquaculture Research & Development

OPEN ACCESS Freely available online

Research Article

Nitazoxanide Activating keap1a/Nrf2 Signaling Pathway is Regulated by *Cul3* of *Criataria plicata*

Wuting Lu, Feixiang Su, Fanhua Yang, Jinhua An, Baoqing Hu, Shaoqing Jian, Gang Yang*, Chungen Wen*

Department of Aquatic Science, Nanchang University, Nanchang, China

ABSTRACT

Cul3 regulates the ubiquitination and degradation of Nrf2 in Nrf2/keap1a pathway under normal conditions. In aquatic invertebrates, the related mechanism of activating oxidative stress in mussels was studied by stimulating *Cristatra plicata* with Nitazoxanide (NTZ). The full-length *Cul3* gene of *C. plicata*, designated *CpCul3* was cloned. The comparative sequence analysis of *CpCul3* gene and its homologous genes showed that *CpCul3* gene was highly similar to the homologous genes of other species in amino acid sequence. The amino acid sequence of *CpCul3* is 78%-98% similar to that of other invertebrates. In the phylogenetic tree, *CpCul3* gene is more closely related to the *Cul3* gene in other bivalves. After NTZ stimulation, the expression level of *CpCul3* mRNA increased in hepatopancreas of the *C. plicata*. The protein expression level of *CpCul3* was detected by utilizing *CpCul3* specific antibody, and the expression level also increased. The results of subcellular localization of *CpCul3* in HEK293T indicated that *CpCul3* could co-locate with mitochondria, lysosomes, and endoplasmic reticulum, and the colocalization with mitochondria is more obvious. The results indicated that *CpCul3* may plays an important role in regulating oxidative stress. The CoIP experiment proved that *CpCul3* could promote the ubiquitination degradation of CpNrf2. Lastly, CpNrf2 could be degraded by K48-mediated ubiquitination.

Keywords: *Cristatra plicata*; *Cul3*; keap1a/Nrf2; Oxidative stress

INTRODUCTION

NTZ is a nitrothiazole benzamide derivative (2-acetyloxy-N-5-nitro-2-thiazolyl), and Jean Francois Rossignol first used it as an insect repellent against liver nematodes and intestinal repair in 1975, has antibacterial and antiviral effects and can inhibit glioma growth by elevated protein levels of ING1, LC3, and SQSTM1 in mouse [1-4]. Nevertheless, excessive use of NTZ can indeed cause oxidative stress damage to cells and the organism. For instance, the increased mitochondrial ROS levels were detected with the extension of NTZ treatment in MGHU3 cells, and the excessive production of ROS is mainly caused by NTZ-mediated mitosis initiation and lysosomal degradation in the later stage [5]. The drug can also induce ROS overproduction, and increased the levels of ROS, CAT, and GSH after the embryos of zebrafish is exposed to NTZ, but inhibited the activity of SOD and CAT [6].

Oxidative stress refers to the excessive production of Reactive Oxygen Species (ROS) and Reactive Nitrogen Species (RNS) in organism while the body is subjected to various harmful stimuli, the dynamic imbalance of the oxidation system and anti-oxidation system leads to tissue damage [7]. Keap1a/Nrf2 signaling pathway plays an important role in oxidative stress, which is activated by non-biological factors such as heavy metal pollution, organic pollutants, drugs, and biological factors such as bacteria, viruses, toxic algae, parasites [6,8-13]. Under physiological conditions, Nuclear Factor E2-related factor 2 (Nrf2) binds to Kelch-like epichlorohydrin-related protein 1 (Keap1) and undergoes ubiquitination system degradation [14]. Under oxidative stress or in the presence of Nrf2 activators, the structure of Nrf2 and Keap1 complex changes, and Nrf2 protein escapes the inhibitory effect of Keap1, and the synthesized Nrf2 accumulates in cytoplasm and enters into nucleus [15], forming heterodimers with the sMaf protein (MafF/MafG/MafK) in nucleus [16]. The heterodimer of Nrf2/sMaf regulates the Antioxidant Response Element (ARE) and activates the body's antioxidant network system, enhancing cellular antioxidant capacity and protecting cells from oxidative damage [17].

Protein ubiquitination is one of the most important post-translational protein modifications, which plays an important role in maintaining intracellular homeostasis and maintains normal cellular physiology, and many cellular functions [18,19]. Human

Correspondence to: Chungen Wen, Department of Aquatic Science, Nanchang University, Nanchang, China, Tel: +86 138 7080 9765; E-mail: cgwen@ncu.edu.cn

Gang Yang, Department of Aquatic Science, Nanchang University, Nanchang, China, Tel: +86 15879116297; E-mail: gangyang@ncu.edu.cn

Received: 11-May-2024, Manuscript No. JARD-24-25658; **Editor assigned:** 15-May-2024, Pre QC No. JARD-24-25658 (PQ); **Reviewed:** 29-May-2024, QC No. JARD-24-25658; **Revised:** 05-Jun-2024, Manuscript No. JARD-24-25658 (R); **Published:** 12-Jun-2024, DOI: 10.35248/2155-9546.24.15.887

Citation: Lu W, Su F, Yang F, An J, Hu B, Jian S, et al (2024) Nitazoxanide Activating keap1a/Nrf2 Signaling Pathway is Regulated by *Cul3* of *Criataria plicata*. J Aquac Res Dev. 15:887.

cells express eight different cullins, *CUL1*, *CUL2*, *CUL3*, *CUL4A*, *CUL4B*, *CUL5*, *CUL7*, and *CUL9*, which have evolutionarily conserved Cullin homologous domains at C-terminus responsible for the interaction between cullin and RBX1 or RBX2 [20]. The Cullin3 (*Cul3*) ubiquitin ligase family consists of three components: the ring finger protein RBX1, the *Cul3* scaffold, and the Bricka bruc/Tramwork/Road complex (BTB) protein, which serves as a connection between *Cul3* and substrates. The human genome encodes approximately 180 BTB proteins, which means a broad ubiquitination signal and substrate library [21]. Keap1 (Kelch ECH associated protein 1) is the first substrate recognition protein reported to bind to Cullin3 in mammalian thin robes, belonging to the BTB Kelch protein family KLHL protein, which binds to Cullin3 through BTB domain and is responsible for binding to substrates through the Ke1ch domain. Classic substrates include NRF2, IKKβ, p62, and so on [22-24].

Cristaria plicata has strong water filtration ability, which is suitable for habitat, with advantages such as fast pearl formation and strong adaptability, and is an important economic species in aquaculture production in China. The shell is utilized as a button, shell carving serves as a raw material for craftsmanship, and is also used as a mother of pearl. The mussel is consumed as a product, shell powder is designated as feed for livestock and poultry, and is a freshwater pearl industry variety [25,26]. The heavy metals, pesticides, and algal toxins in water environment, affect the survival of mussels. The Keap1/Nrf2 signaling pathway is considered to be the main defense mechanism against cellular oxidative stress. During individual growth, exogenous stimuli can disrupt the cellular oxidative pathway and trigger this signaling pathway [27].

In the present study, we focused on the function of *C. plicata* *CpCul3* and its regulating effect on Keap1-Nrf2/ARE signal pathway. After NTZ stimulation, the mRNA and protein expression levels of *CpCul3* were significantly increased in hepatopancreas of the mussel. The subcellular localization results of *CpCul3* in HEK293T indicated that it could co-localize with mitochondria, lysosomes, and endoplasmic reticulum. Moreover, Cp*Cul3* could also promote the ubiquitination degradation of CpNrf2, and the promoter activity of Cp*Cul3* is regulated by CpNrf2 and CpMafk.

MATERIALS AND METHODS

Animals and cells

Healthy *Cristaria plicata* is collected from Anhui Shuiyun Environmental Protection Co., Ltd in Wuhu, China. The mussels were acclimated for one week at 25°C-30°C with filtered, aerated freshwater. HEK293T cells were grown at 37°C and 5% CO_2 with DMEM (C3103-0500, VivaCell) supplemented with 10% fetal bovine serum (C04001-500, VivaCell) and 1% penicillin-streptomycin (Sangon Biotech, China).

Immune stimulation and sample collection

Nitazoxanide (99%, CAS: 55981-09-4) was obtained from Yuanye Biotechnology Co. Ltd (Shanghai, China). 18 mussels were randomly divided into two groups, one group was exposed to 0.3 mg/L NTZ, and another was in equal DMSO. The hepatopancreas tissue was used to extract total RNA or total protein from each group at 4 days poststimulation. The hemolymph from two groups was stained with a Reactive Oxygen Species Assay Kit (Beyotime, S0033S) and was analyzed by a BD LSRFortessa flow cytometer.

cDNA cloning and sequence analysis of *CpCul3*

The full-length cDNA fragments of *CpCul3* were amplified by nested PCR according to the previous report, the primers were designed according to the transcriptome database of our lab [28]. Multiple sequence alignment was constructed with Clustalx from EMBL (www. https://www.ebi.ac.uk/Tools/msa/clustalo/). The protein structure was predicted with SMART (http://smart.embl-heidelberg.de/). I-TASSER online software (https://seq2fun.dcmb.med.umich.edu//I-TASSER/) and Swiss-PdbViewer (https://spdbv.unil.ch/) predicted the protein 3D structure. A phylogenic tree was constructed with the MEGA 11 software using the neighbor-joining method based on an amino acid alignment. *Cul3* sequences from other species were obtained from NCBI (https://www.ncbi.nlm.nih.gov/).

dsRNAi assay

The primers T7- *CpCul3*-F and T7- *CpCul3*-R with T7 promoter sequence were used to amplify *CpCul3* fragment. Then, it was used to synthesize dsRNA of *CpCul3* (604 up). The corresponding control GFP (657 bp) dsRNA was synthesized with the primers T7-EGFP-F and T7-EGFP-R from the pEGFP-C1 vector. The dsRNA was first injected into the mussels at 2 μg of dsRNA per gram of body weight with a microliter syringe through adductor muscle. The mussels were repeatedly injected the equal dsRNA 24 hrs later. The injection volume of the dsRNA solution was adjusted to 100 μL with RNA-free water. The hepatopancreas of each group were collected for the subsequent experiment at 24 hrs after the second injection.

Gene expression profile analysis

The relative expression levels of *CpCul3* and antioxidant-related genes in hepatopancreas of the mussels were determined SYBR Green fluorescent RT-qPCR (Vazyme, Nanjing, China) on a CFX96 Real-Time System (Bio-Rad) with specific primers. PCR conditions were 95°C for 2 min, followed by 40 cycles at 95°C for 5 sec, 58°C for 30 sec, and 72°C for 30 sec, and then melting from 65°C to 95°C. The β-actin gene was utilized as an internal control gene of cDNA standardization. The acquired data was analyzed by the 2-ΔΔCt method. Three independent experiments were carried out and the results were expressed as the mean ± SD.

Subcellular localization

HEK-293T cells were passed into confocal culture dishes, after 12-24 hrs, cells were transfected with indicated plasmids. At 36 hrs post-transfection, the cells were washed twice with PBS and were stained with Mito-Tracker, ER Tracker Red Kit, or Lyso-Tracker Red (Beyotime). Subsequently, Hoechst 33258 solution (Beyotime, China) was applied to stain the nucleus. The treated cells were photographed under a laser scanning confocal microscope (Leica SPE).

Dual-luciferase report gene assays

For investigating the influence of CpNrf2: MafK on *CpCul3* gene expression, dual-luciferase report gene assays were executed. The approximate 1 × 105 HEK293T cells seeded in 24 well plates were grown to 70%-80% confluent and transiently co-transfected with 250 ng pGL3-*CpCul3* plasm, 50 ng pRL-TK reporter plasmid (Promega) and 250 ng pCDNA3.1-CpNrf2 or pCDNA3.1-

CpMafk. To detect the role of bZIP domain on the activity of *CpCul3* promoter, the p3xFLAG-14-bZIP plasmid was transfected to cells. Cells transfected with pcDNA3.1 or p3xFLAG-14 plasmid were used as control. Luciferase activity was measured by the Dual-Luciferase Reporter Assay System (Promega). Data was obtained from three independent experimental samples in triplicate.

Immunoblotting

Cells or fresh hepatopancreas tissues were lysed in cold RIPA buffer added with protease inhibitor (20124ES03, Yeasen) in advance. The lysates were centrifuged at max speed (14000 rpm) for 15 min at 4°C. Protein concentration was determined by the BCA protein assay kit (C503021-0501, Sangon). An equal amount of protein (30 μg-50 μg) was analyzed using 10% SDS-PAGE gel and transferred onto PVDF filter membrane. The membrane was blocked with 5% nonfat milk in Tris-Buffered Saline (TBS) (20 mM Tris-HCl, pH 8.0, 150 mM NaCl) for 1-1.5 hrs then incubated with the rabbit anti-*CpCul3* (1:4000) overnight at 4°C. After three washes with TBST, the PVDF membranes were incubated with Mouse Anti-Rabbit IgG LCS (A25022, Abbkine). The proteins were detected by the ECL method on the Bio-Rad imaging system.

Co-IP

HEK293T cells were seeded in 10 cm dishes (1 × 107 cells/dish) for 12-24 hrs to form a monolayer of cells that is 70% to 90% confluent. The cells were transfected with indicated plasmids. At 36 hrs post-transfection, the medium was removed carefully, and the cell was washed twice with ice-cold PBS. The cells were then lysed with Cell lysis buffer (P0013, Beyotime) for 30-40 min at 4°C. Lysates were centrifuged at 14,000 rpm for 15 min. The supernatant was incubated with control IgG or Anti-GFP tag nanobody-coated Agarose beads (KTSM1301, AlpaLifeBio). Wash beads 4 times with washing buffer (50 mM Tris-HCl, pH 7.4, 150 mM NaCl, 1 mM EDTA, 1 mM EGTA). Eluting immunoprecipitated proteins from the beads adding 100 μL of 2 × SDS loading buffer and boiling the beads in a thermal block set at 98°C for 10 min. The resin mixture was centrifuged at 2500 × gm for 5 min. The supernatant was evaluated by SDS-PAGE.

Immunohistochemistry

The tissues of hepatopancreas were fixed in 4% paraformaldehyde and were embedded in paraffin blocks. Then the paraffin was cut into 5 μm. The antigen was restored with a Citric acid antigen repair solution (G1202-250 ML, ServiceBio). The sections were incubated in 0.5% Triton X-100 in PBS for 60 min at RT (Room Temperature). The non-specific signal was blocked using 3% BSA for 1 hr in 0.5% Triton X-100. Hepatopancreas samples were stained with *CpCul3* antibody overnight at 4°C and were incubated with 488 fluorescent second antibody. The slides were incubated with an organic spontaneous fluorescence quencher and mounted with a mounting medium. Finally, the slides were imaged with confocal microscopy and were evaluated with fluorescence intensity.

CpCul3 antibody production

The last 597 bp of *CpCul3* Open Reading Frame (ORF) sequence was amplified and was ligated into the expression vector pET-28a(+) with 6xHis-tag. The valid recombinant plasmid was extracted and transformed into *E. coli* BL21 (DE3) Chemically competent cell (TSC-E05, Tsingke, China). A positive colony was induced by Isopropyl-β-D-Thiogalactose (IPTG) and the protein was purified by Ni-NTA resin. The purified protein was concentrated and quantified with a BCA protein assay kit (Thermo Fisher, USA). To acquire the anti-*CpCul3* Ab, that was mixed 0.5 ml of purified *CpCul3* protein (1 mg/ml) with an equal volume of Freund's Complete Adjuvant (FCA) to immunize the New Zealand white rabbit. Half of the antigen was used with Freund's incomplete adjuvant in the next three immunizations. The serum was tested after the third immunization. Rabbits were sacrificed to obtain the antiserum 7 days after the fourth immunization. Hereafter, the Ab was purified by using a protein A resin column. To prove the effectiveness of the Ab, Western blotting was utilized to detect *CpCul3* protein in hepatopancreas through anti-*CpCul3*, and a single band at the position of 90 kDa for the target was found.

Statistical analysis

The statistical analysis was performed using Student's t-test or one-way Analysis of Variance (ANOVA), and the data were presented as mean ± SD from 3 independent experiments. Significance was accepted at $P<0.05$ (*$P<0.05$, **$P<0.01$, ***$P<0.001$, ****$P<0.0001$).

RESULTS

Complementary DNA cloning and bioinformatics analysis of *Cul3*

The full-length *CpCul3* Complementary DNA (cDNA) was cloned from hepatopancreas. The *CpCul3* contained a 237 bp 5′ UTR, an 878 bp 3′ UTR, and an ORF. The ORF encoded an 88.7 kDa protein comprising 762 amino acids. Similar to other vertebrates and invertebrates, *CpCul3* protein also contained SCOP-d1ldja2, CULLIN, and Nedd8 domains (Figure 1). Additionally, the lengths of ORFs were the same (Figures 1A and 1D). As predicted by the SWISS model, *CpCul3* shared high similarity with the tertiary structure of Danio rerio *Cul3* (Figure 1B). To further explore the evolutionary relationship of *Cul3*, the amino acid sequence was used to construct a phylogenetic tree. The mammalian *Cul3* clustered into a clade with the homologs in reptiles, gastropods, arthropods, bony fish, and bivalves. The clustering of *CpCul3* with its homologs in other various species indicates their close evolutionary relationship (Figure 1C).

Tissue-specific expression of *CpCul3*

CpCul3 was expressed in all tested mussel tissues, including hepatopancreas and kidney. To further determine the protein expression level of *CpCul3* in various tissues of mussels, *CpCul3* proteins and synthesized Rabbit polyclonal antibody against *CpCul3* was constructed. Western blot assay suggested that *CpCul3* was highly expressed in hepatopancreas, kidney, and muscle tissue, while the expression was lower in hemolymph (Figure 2).

Participation of *CpCul3* in the immune response

The reactive oxygen species in hemolymph increased approximately three times after NTZ exposure (Figure 3A). In hepatopancreas, the expression of *CpCul3* was significantly upregulated at 12 hrs, 36 hrs, and 96 hrs after NTZ stimulation (Figure 3B). Meanwhile, *CpCul3* mRNA levels were significantly induced in hepatopancreas after NTZ stimulation at 96 hrs (Figure 3C). *CpCul3* protein expression was significant in hepatopancreas cytoplasm. In addition, the fluorescence intensity in NTZ exposure group was stronger than that in the control group (Figures 3D and 3E).

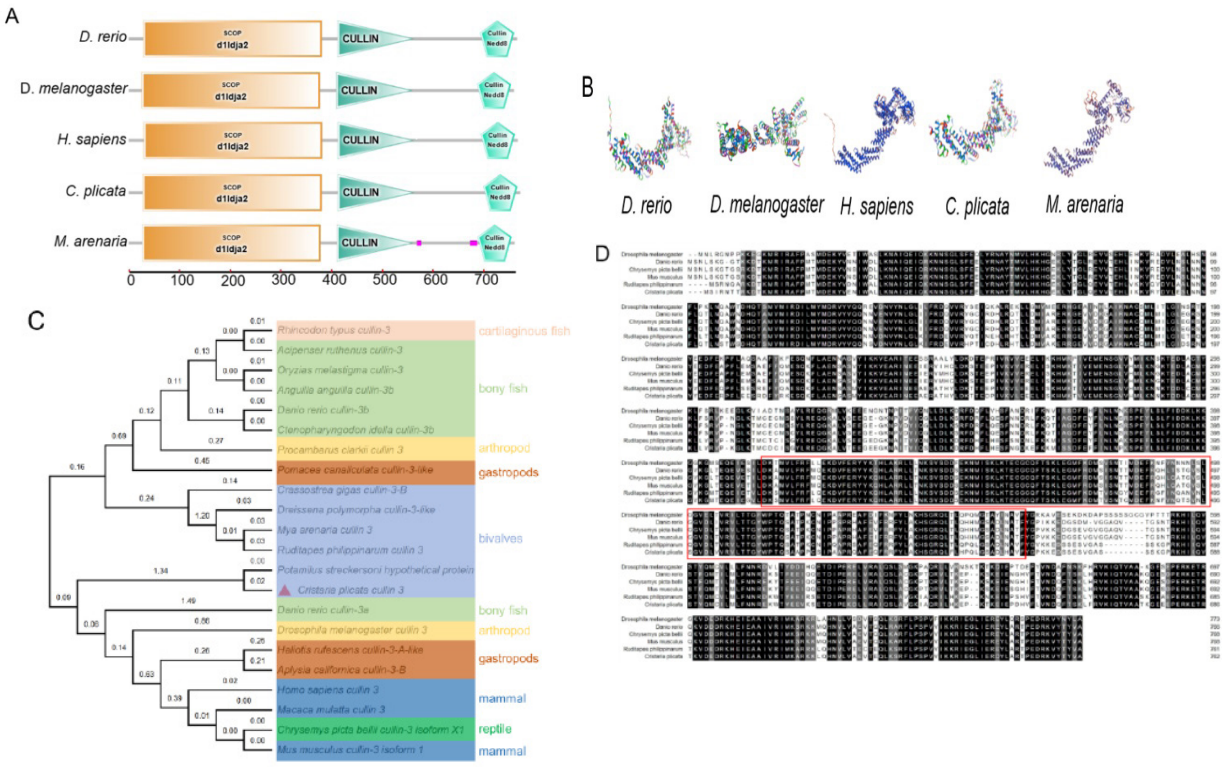

Figure 1: A) Diagram of the domain architectures of Cul3 proteins from *Danio rerio, Drosophila melanogaster, Homo sapiens*, C. *plicata*, and M*ya arenaria*; B) A comparison of the 3D structures of Cul3 proteins from the aforementioned species; C) Phylogenetic trees of C*ul3* from the indicated species were constructed *via* the Mega 11 software and based on multiple sequence alignment by Clustal W. Bootstrap values of 1000 replicates (%) are indicated for the branches; D) Phylogenetic trees of C*ul3* from the indicated species were constructed *via* the Mega 11 software and based on multiple sequence alignment by Clustal W. Bootstrap values of 1000 replicates (%) are indicated for the branches.

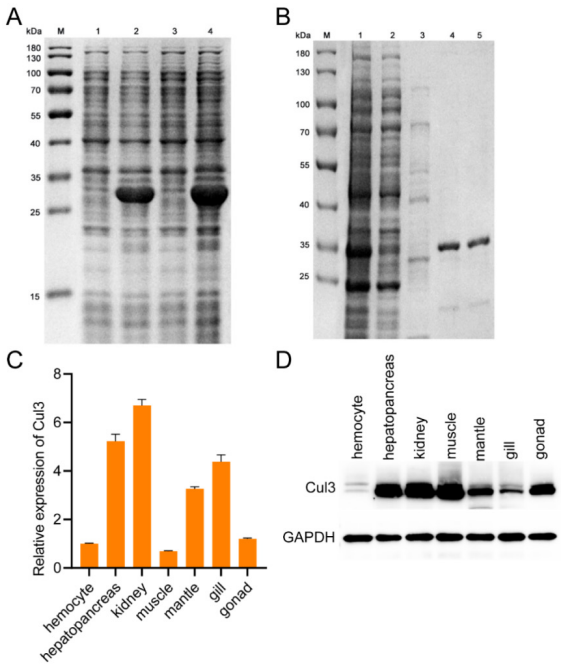

Figure 2: mRNA and protein expression level of C*pCul3* in various tissues. **Note:** A) Constructs pET30a (+)-C*pCul3* were transformed into *E. coli* and the expression of proteins was induced by IPTG and was analyzed by SDS-PAGE. Where, Lane M-Protein markers, Lane 1 and Lane 3-Protein from *E. coli* with pET30a (+)-C*pCul3* without IPTG induction, Lane 2 and Lane 4-Protein from *E. coli* with pET30a (+)-C*pCul3* with IPTG induction at 37°C or 16°C; B) Protein from *E. coli* with pET30a (+)-C*pCul3* with IPTG induction at 16°C and was purified with nickel column. Where, Lane M-Protein markers, Lane 1-Supernatant, Lane 2-Flowing fluid, Lane 3-5-Eluent; C) Expression of C*pCul3* in the indicated tissues was determined by qPCR. The data was representative of three independent experiments; D) Western blot detection of the tissue distribution of C*pCul3*, GAPDH was regarded as the reference.

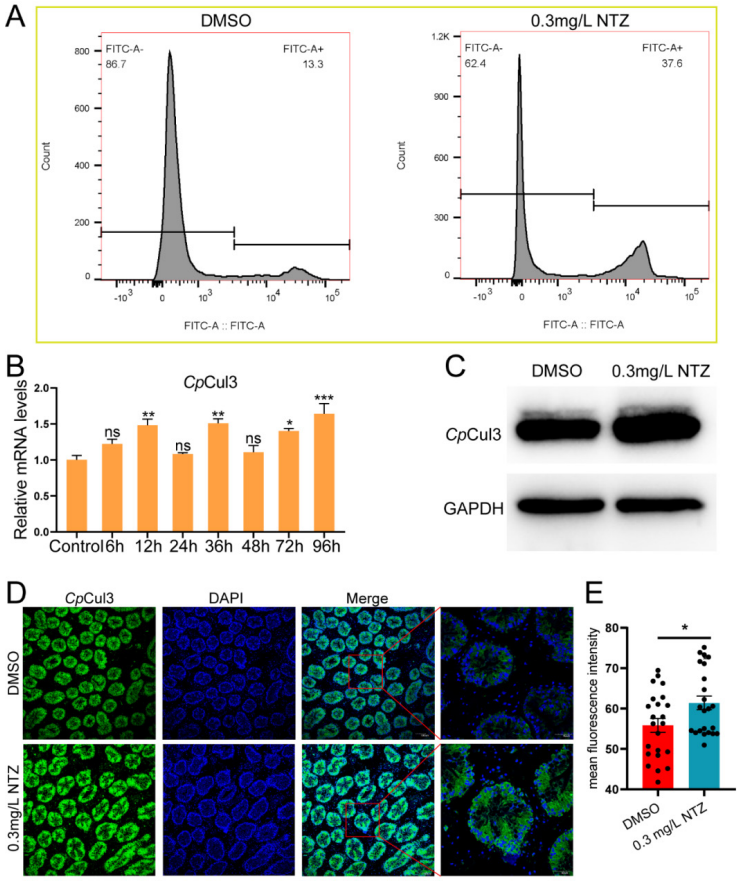

Figure 3: ROS detection hemolymph and the expression changes of *CpCul3* after NTZ stimulation in hepatopancreas. **Note:** A) FITC-A+ represented the DCFH-DA probe labeled hemolymph. The FITC-A+ cells were increased after NTZ stimulation and DMSO was used as a control; B) The mRNA expression of *CpCul3* after NTZ stimulation at a designated time. ns: no significant difference. Where, (*)-P<0.05, (**)-P<0.01, (***)-P<0.01; C) The protein expression of *CpCul3* after NTZ stimulation for 96 hrs in hepatopancreas; D) Fluorescent immunohistochemistry in hepatopancreas from 0.3 mg/L NTZ exposure group and control group. It showed anti-*CpCul3* positive. The scale bar was 40 μm; E) The statistical analysis of fluorescence intensity from Figure 3D (n=23), where, (*)-P<0.05.

Subcellular localization of *CpCul3* in HEK293T cells

HEK293T cells were used to investigate the subcellular localization of *CpCul3* proteins. As shown in Figure 4, *CpCul3*-GFP fusion protein was localized in cytoplasm, and had a colocalization with mitochondria, lysosomes, endoplasmic reticulum (Figures 4A-4C).

Interaction of *CpCul3* with *Cp*RBX1 and *Cp*keap1a

CpCul3 interacts with CpRBX1 and Cpkeap1a, respectively the subcellular localization results in HEK293T indicated that *CpCul3* had localization with CpRBX1 and Cpkeap1a. Co-IP assays showed that *CpCul3* could interact with Cpkeap1a and CpRBX1 (Figure 5).

Regulation of *CpCul3* by Nrf2/Mafk pathway

A 2512 bp *CpCul3* promoter sequence was cloned and had Nrf2, MafK, and MakG binding sites. In CpNrf2 or CpMafk-transfected HEK293T cells, *CpCul3* promoter activation was inhibited after NTZ stimulation (Figure 6A). Nrf2 interacts with Mafk through its bZIP domain [29]. In CpNrf2 and CpMafk co-transfected HEK293T cells, *CpCul3* promoter activation was inhibited, which were similar to bZIP and CpMafk co-transfected HEK293T cells (Figure 6B). Afterwards, plasmid-protein complexes containing CpMafk fusion proteins and *CpCul3* pro-Luc had slower migration rate that was more slowly with the increase of protein concentration (Figure 6C). The results indicated that CpNrf2/Mafk could bind to *CpCul3* promoter.

The expression of antioxidant genes were regulated by *CpCul3*

While *CpCul3* was disturbed with double-strand RNA, The expression of *CpCul3* was significantly inhibited. The expression level of CAT, GST, and SOD mRNA decreased, while Nrf2, keap1a, and NQO1 relatively increased. The expression of antioxidant genes (CAT, GPX1, Hmox1, NQO1, NFE2L2, PRDX1, SOD1, and SOD2) obviously reduced after the overexpression of *CpCul3* in HEK293T cells (Figure 7).

The ubiquitination of CpNrf2

The plasmid FLAG-*CpCul3* was co-transfected with the plasmids HA-Ub and GFP-CpNrf2. The result suggested that *CpCul3* facilitated the ubiquitination by CpNrf2 (Figure 8A). The plasmid GFP-CpNrf2 was co-transfected with the plasmids HA-Ub or HA-Ub-K48. The results of immunoprecipitation showed that CpNrf2 could be ubiquitinated by K48-mediated ubiquitination (Figure 8B).

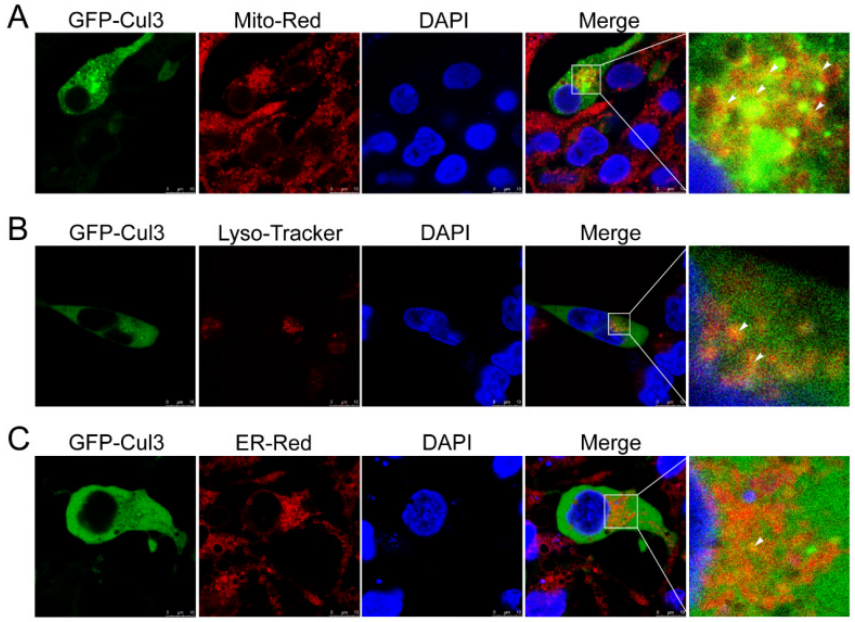

Figure 4: Cellular localization of *CpCul3* in HEK293T. **Note:** The co-localization of *CpCul3*-GFP with A)-Red mitochondria; B)-Red lysosomes; and C)- Red endoplasmic reticulum, respectively. DAPI was used to stain the nucleus. The white arrowhead indicated the overlap of green and red.

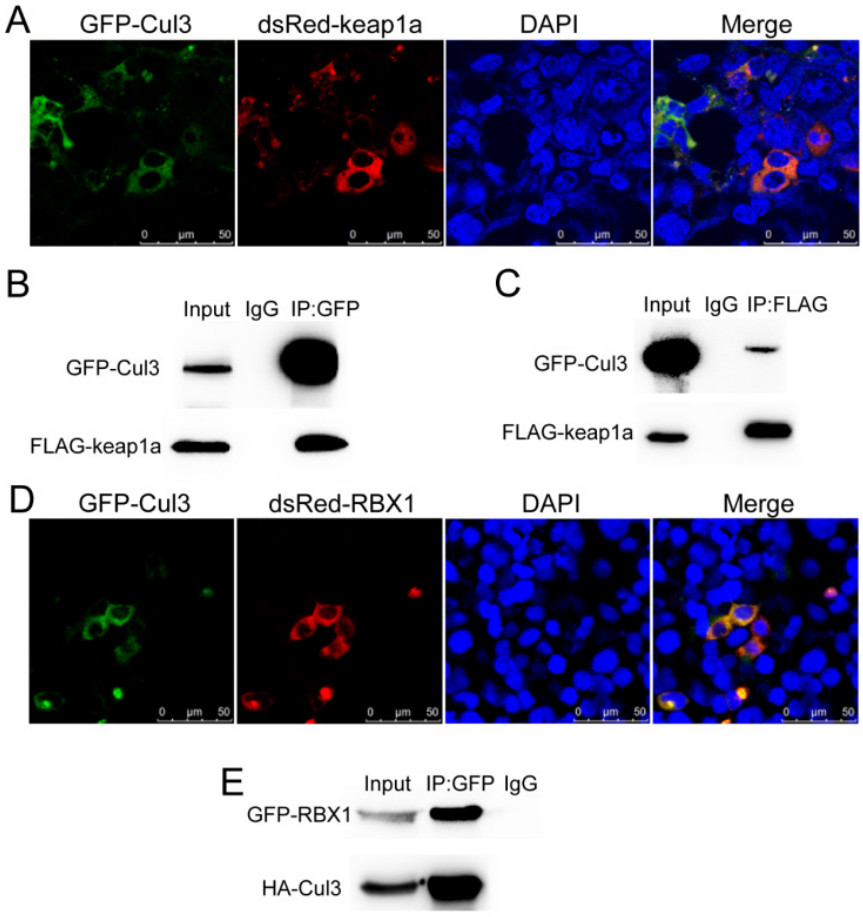

Figure 5: Interaction of *CpCul3* with Cpkeap1a and CpRBX1. **Note:** A,D) Colocalization of *CpCul3* with Cpkeap1a and CpRBX1 in HEK293T cells by confocal analysis; B,C) Coimmunoprecipitation assay results showing the interaction between *CpCul3* and Cpkeap1a in HEK293T cells. Anti-GFP and anti-FLAG antibodies were utilized to detect *CpCul3* and Cpkeap1a in co-transfected HEK293T cells, respectively; E) 293T cells were co-transfected with HA-*CpCul3* and GFP-CpRBX1, followed by Co-IP assay with anti-HA or anti-GFP antibody. All experiments were repeated at least three times.

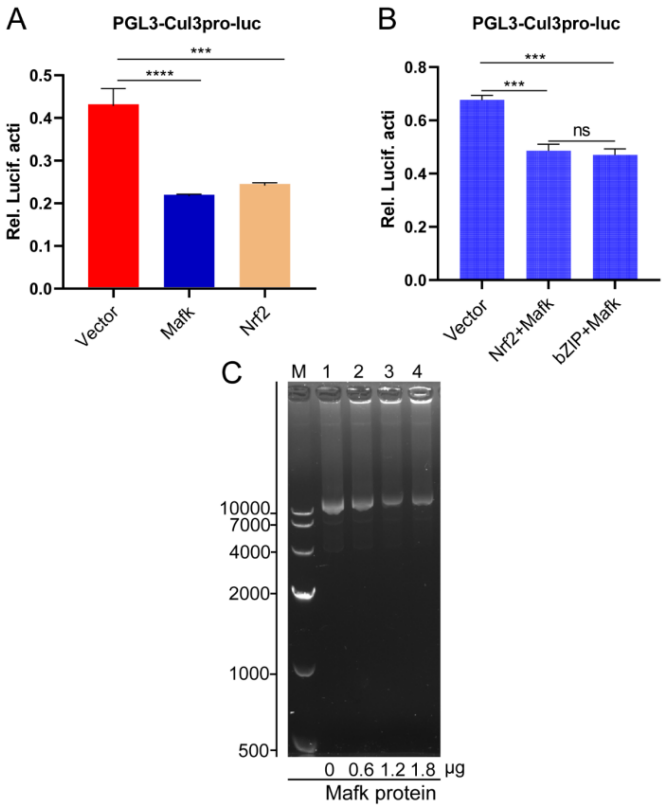

Figure 6: Transcriptional regulatory function of *CpCul3*. **Note:** A,B) HEK293T cells were cotransfected with CpNrf2 or CpMafk or CpbZIP and *CpCul3* promoter constructs for 36 hrs, followed by stimulation with NTZ, or mock transfection for 36 hrs. Cells were then collected and subjected to luciferase analysis; C) *CpCul3* promoter plasmid was incubated with CpMafk recombinant protein and conducted agarose gel electrophoresis. A) (■): Vector, (■)-Mafk, (■)-Nrf2; B) (■)-Vector, Nrf2+Mafk, bZIP+Mafk at different phases.

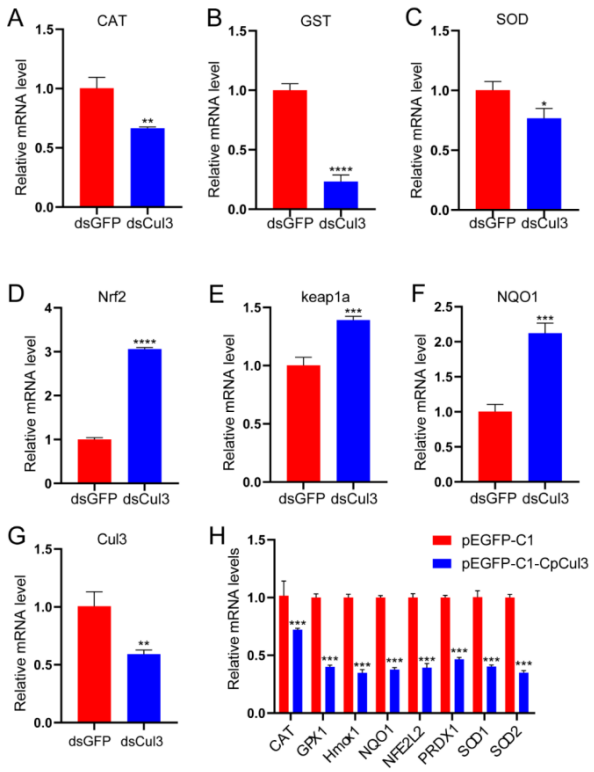

Figure 7: Interference and overexpression of *CpCul3*. **Note:** A-G) RNAi of the expression of the antioxidant-related gene in hepatopancreas; dsGFP served as the control. Three mussels were used to prepare each sample, and the data are representative of three independent experiments; H) HEK293T cells were transfected with a GFP vector or GFP-*CpCul3* and the mRNA levels of antioxidant-related genes were monitored by qPCR. (■)-pEGFP-C1, (■)-pEGFP-C1-*CpCul3*.

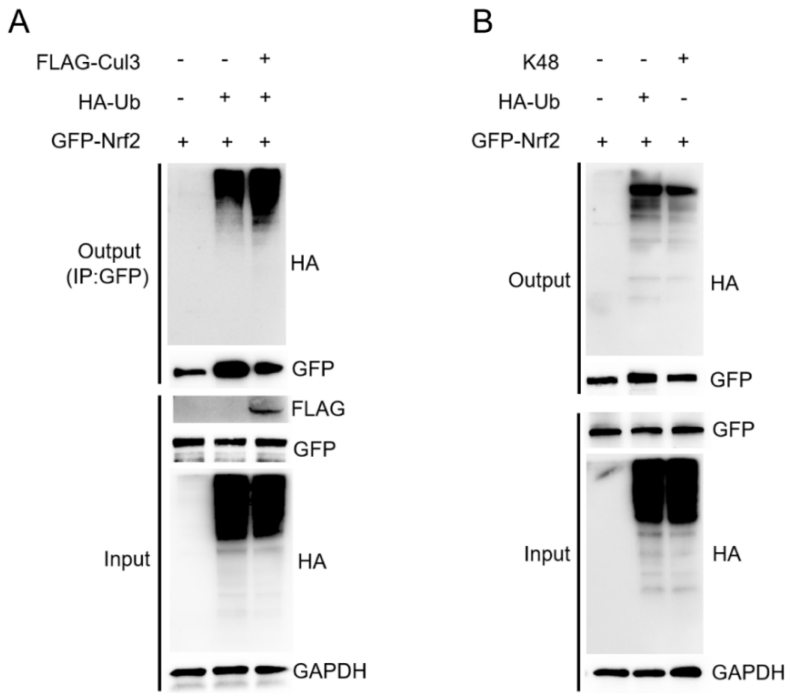

Figure 8: CpNrf2 is ubiquitinated. **Note:** A) 293T cells were co-transfected with pGFP-CpNrf2 and pHA-Ub, together with pFlag-C*p*C*ul3*. The cells were lysed and analyzed by Co-IP assays with anti-GFP antibody; B) HEK293T cells seeded in 10 cm2 dishes were transfected with pGFP-CpNrf2, together with Ub-WT or Ub-K48. The ubiquitination of CpNrf2 was determined by western blotting using the corresponding tag Abs.

DISCUSSION

Cul3 is evolutionarily highly conservative, and it contains typical CULLIN and Nedd8 domains [30]. The activity of CRLs (Cullin-RING Ligases) is regulated by post-translational modifications of Nedd8, and these covalent modifications are necessary for the connection between the Cullin protein and the E2 binding enzyme, prompting E3 ligases that recruit ubiquitin molecules to perform ubiquitination modifications on specific substrates [30]. The comparative sequence analysis of C*pCul3* gene of *C. plicata* with its homologs showed that C*pCul3* gene had a high similarity with its homolog genes of other species in amino acid sequences. The amino acid sequence of C*pCul3* shared 78%-98% similarity with that of other invertebrates. C*pCul3* gene also had conservative CULLIN and Nedd8 domains. In the phylogenetic tree, C*pCul3* gene was closely related to *Cul3* in other bivalves, such as *Potamilus streckersoni* and *Mya arenaria*. It was speculated that the function and role of *Cul3* might also be conservative in evolution.

In mammals, *Cul3* is widely expressed in hepatopancreas, brain, kidney, and ovary [31-34]. The high expression of C*pCul3* was detected in hepatopancreas, kidney, and muscle. The tissue of hepatopancreas is an important immune organ of mollusks and plays an important role in immune responses. The relatively high expression levels of C*pCul3* in hepatopancreas suggested that it might be involved in the immune process and regulated the expression of immune-related genes. Therefore, the expression level of C*pCul3* mRNA in hepatopancreas increased after NTZ stimulation. Meanwhile, C*pCul3* antibody was employed to examine the above result under the protein level, which was similar to that of mammals [35]. The above data showed that *C. plicata* had an evolutionarily conserved *Cul3*, and might have an immunosuppressive function similar to its mammalian homologs.

In human renal tubular epithelium, *Cul3* can co-localize with mitochondria and directly interact with MRPL12 to induce K63-associated ubiquitination of MRPL12, leading to mitochondrial biosynthesis dysfunction [36]. *Cul3* is probably involved in the regulation of endosome maturation through ubiquitination, the absence of *Cul3* leads to the deformation of endosomes and the defect of endocytosis transport to lysosomes, and *Cul3* plays an important role in the later stage of regulating the transport route of lysosomes [37]. The endoplasmic reticulum is the largest membrane-bound organelle in eukaryotes, and it is a continuous structure extending from the nuclear membrane to the plasma membrane [38,39]. The endoplasmic reticulum interacts closely with many organelles, including mitochondria, Golgi apparatus, endosomes, lysosomes, peroxisomes, and plasma membranes, so that lipids and intracellular signals can be transmitted [40]. The endoplasmic reticulum-forming protein Lunapark is ubiquitinated by CRL3klhl12 ubiquitin ligase. Inhibition of Lunapark ubiquitination can lead to neural development defects, and KLHL12-dependent Lunapark ubiquitination is necessary for normal growth and development [41]. The above research shows that *Cul3* has a close functional relationship with intracellular organelles. The results of subcellular localization of C*pCul3* in HEK293T exhibited that C*pCul3* could also co-locate with mitochondria, lysosomes, and endoplasmic reticulum, especially with mitochondria, which is the main structure of cells participating in oxidative stress, indicating that C*pCul3* might play an important role in regulating the oxidative stress process.

Cul3, keap1, and RBX1 form a complex to conduct the ubiquitination degradation in cytoplasm, the amino-terminal of *Cul3* is connected with keap1 [42], and its carboxyl end interacts with RBX1 [20]. Both subcellular localization and CoIP proved that C*pCul3* could interact with Cpkeap1a and CpRBX1, respectively. This indicated that the ubiquitination system was conservative in evolution. Under normal circumstances, Nrf2 is ubiquitinated and

degraded in the cytoplasm. The up-regulation of *Cul3* can promote the ubiquitination of its substrate, *CpCul3* was co-transfected into HEK293T cells with CpNrf2, and the result showed that the ubiquitination level of CpNrf2 also increased [36]. *Cul3* ubiquitin ligase can mediate the degradation of K48 polyubiquitination of its substrate CoIP experiment proved that CpNrf2 could indeed undergo K48-linked polyubiquitination in HEK293T cells [43].

CONCLUSION

As *Cul3* can control the ubiquitination of its substrates, we further explored its regulation of the oxidative stress pathway (keap1-Nrf2) through interference and over-expression. Fluorescence quantitative PCR data revealed that the expression levels of antioxidant genes were changed after interfering with *CpCul3* in hepatopancreas of *C. plicata* and overexpressing *CpCul3* in HEK293T cells, this result suggested that *CpCul3* had a regulatory effect on keap1-Nrf2 pathway, and the double luciferase experiment further verified the negative feedback regulation effect of CpNrf2 on *CpCul3* under NTZ stimulation. The above results indicated that *CpCul3* played an essential role in keap1-Nrf2 pathway.

In summary, *CpCul3* was highly conserved in evolution and widely expressed in various tissues of *Cristaria plicata*. The *CpCul3* mRNA and protein expression levels increased under NTZ stimulation. *CpCul3* could promote the ubiquitination of CpNrf2. CpNrf2 and CpMafk could bind to the promoter of *Cul3* to regulate the expression of *CpCul3*.

ACKNOWLEDGMENTS

Funding

This research was financially supported by grants (No. 331460697, 13007168, 13007198) from the National Natural Science Foundation of China, the Support Project of the Modern Agricultural Industry Technology System (ZQT20180027), the Scientific and Technological in Jiangxi Province (20160BBF60053, 20192BAB204009), the Jiangxi Agriculture Research System (JXARS-03).

Credit authorship contribution statement

Wuting Lu: Investigation, conceptualization, methodology, formal analysis, writing-original draft; Feixiang Su: Validation, resources; Fanhua Yang: Laser confocal photography; Jinhua An: Software, data curation; Baoqing Hu: Investigation, funding acquisition; Shaoqing Jian: Validation, methodology. Gang Yang: Supervision; Chungen Wen: Writing-review and editing, supervision, funding acquisition.

Conflict of interest

The authors of this article declare no conflict of interest.

REFERENCES

1. Fox LM, Saravolatz LD. Nitazoxanide: A new thiazolide antiparasitic agent. Clin Infect Dis. 2005;40(8):1173-1180.
2. Dubreuil L, Houcke I, Mouton Y, Rossignol JF. *In vitro* evaluation of activities of nitazoxanide and tizoxanide against anaerobes and aerobic organisms. Antimicrob Agents Chemother. 1996;40(10):2266-2270.
3. Al-Kuraishy HM, Al-Gareeb AI, Elekhnawy E, Batiha GE. Nitazoxanide and COVID-19: A review. Mol Biol Rep. 2022;49(11):11169-11176.
4. Wang X, Shen C, Liu Z, Peng F, Chen X, Yang G, et al. Nitazoxanide, an antiprotozoal drug, inhibits late-stage autophagy and promotes ING1-induced cell cycle arrest in glioblastoma. Cell Death Dis. 2018;9(10):1032.
5. Sun H, Ou T, Hu J, Yang Z, Lei Q, Li Y, et al. Nitazoxanide impairs mitophagy flux through ROS-mediated mitophagy initiation and lysosomal dysfunction in bladder cancer. Biochem Pharmacol. 2021;190:114588.
6. Lu W, Yang F, Meng Y, An J, Hu B, Jian S, et al. Immunotoxicity and transcriptome analysis of zebrafish embryos exposure to Nitazoxanide. Fish Shellfish Immunol. 2023;141:108977.
7. Cai L, Kang YJ. Oxidative stress and diabetic cardiomyopathy: A brief review. Cardiovasc Toxicol. 2001;1(3):181-193.
8. Liu J, Liao G, Tu H, Huang Y, Peng T, Xu Y, et al. A protective role of autophagy in Pb-induced developmental neurotoxicity in zebrafish. Chemosphere. 2019;235:1050-1058.
9. Wang Q, Gu X, Liu Y, Liu S, Lu W, Wu Y, et al. Insights into the circadian rhythm alterations of the novel PFOS substitutes F-53B and OBS on adult zebrafish. J Hazard Mater. 2023;448:130959.
10. Jiang WD, Hu K, Liu Y, Jiang J, Wu P, Zhao J, et al. Dietary myo-inositol modulates immunity through antioxidant activity and the Nrf2 and E2F4/cyclin signalling factors in the head kidney and spleen following infection of juvenile fish with *Aeromonas hydrophila*. Fish Shellfish Immunol. 2016;49:374-386.
11. Singh E, Matada GSP, Abbas N, Dhiwar PS, Ghara A, Das A. Management of COVID-19-induced cytokine storm by Keap1-Nrf2 system: A review. Inflammopharmacology. 2021;29(5):1347-1355.
12. Falfushynska H, Horyn O, Osypenko I, Rzymski P, Wejnerowski L, Dziuba MK, et al. Multibiomarker-based assessment of toxicity of central European strains of filamentous cyanobacteria *Aphanizomenon gracile* and *Raphidiopsis raciborskii* to zebrafish *Danio rerio*. Water Res. 2021;194:116923.
13. Zhou W, Quan JH, Lee YH, Shin DW, Cha GH. *Toxoplasma gondii* proliferation require down-regulation of host nox4 expression *via* activation of PI3 Kinase/Akt signaling pathway. PLoS One. 2013;8(6):e66306.
14. Kobayashi A, Kang MI, Okawa H, Ohtsuji M, Zenke Y, Chiba T, et al. Oxidative stress sensor Keap1 functions as an adaptor for *Cul3*-based E3 ligase to regulate proteasomal degradation of Nrf2. Mol Cell Biol. 2004;24(16):7130-7139.
15. Yang Y, Cvekl A. Large Maf transcription factors: Cousins of AP-1 proteins and important regulators of cellular differentiation. Einstein J Biol Med. 2007;23(1):2-11.
16. Katsuoka F, Yamamoto M. Small Maf proteins (MafF, MafG, MafK): History, structure and function. Gene. 2016;586(2):197-205.
17. Pellegrino S, Ronda L, Annoni C, Contini A, Erba E, Gelmi ML, et al. Molecular insights into dimerization inhibition of c-Maf transcription factor. Biochim Biophys Acta. 2014;1844(12):2108-2115.
18. Ciechanover A. The ubiquitin-proteasome pathway: On protein death and cell life. EMBO J 1998;17(24):7151-7160.
19. Hershko A, Ciechanover A. The ubiquitin system. Annu Rev Biochem. 1998;67:425-479.
20. Zheng N, Schulman BA, Song L, Miller JJ, Jeffrey PD, Wang P, et al. Structure of the *Cul1*-Rbx1-Skp1-F boxSkp2 SCF ubiquitin ligase complex. Nature. 2002;416(6882):703-709.
21. Chen RH. Cullin 3 and its role in tumorigenesis. Adv Exp Med Biol. 2020;1217:187-210.
22. Cullinan SB, Gordan JD, Jin J, Harper JW, Diehl JA. The Keap1-BTB protein is an adaptor that bridges Nrf2 to a *Cul3*-based E3

ligase: Oxidative stress sensing by a *Cul3*-Keap1 ligase. Mol Cell Biol. 2004;24(19):8477-8486.

23. Lee DF, Kuo HP, Liu M, Chou CK, Xia W, Du Y, et al. KEAP1 E3 ligase-mediated downregulation of NF-kappaB signaling by targeting IKKβ. Mol Cell. 2009;36(1):131-140.

24. Lee Y, Chou TF, Pittman SK, Keith AL, Razani B, Weihl CC. Keap1/Cullin3 modulates p62/SQSTM1 activity *via* UBA domain ubiquitination. Cell Rep. 2017;19(1):188-202.

25. Lecoeur S, Videmann B, Berny P. Evaluation of metallothionein as a biomarker of single and combined Cd/Cu exposure in *Dreissena polymorpha*. Environ Res. 2004;94(2):184-191.

26. Li D, Pan B, Chen L, Wang Y, Wang T, Wang J. et al. Bioaccumulation and human health risk assessment of trace metals in the freshwater mussel *Cristaria plicata* in Dongting Lake, China. J Environ Sci. 2021;104:335-350.

27. Lushchak VI. Environmentally induced oxidative stress in aquatic animals. Aquat Toxicol. 2011;101(1):13-30.

28. Cao X, Lu W, Gang Y, Hu B, Wen C. Prx5 of *Cristaria plicata* has antioxidant function and is regulated by Nrf2/ARE signaling pathway. Fish Shellfish Immunol. 2023;134.

29. Otsuki A, Yamamoto M. Cis-element architecture of Nrf2-sMaf heterodimer binding sites and its relation to diseases. Arch Pharm Res. 2020;43(3):275-285.

30. Wu JT, Lin HC, Hu YC, Chien CT. Neddylation and deneddylation regulate Cul1 and Cul3 protein accumulation. Nat Cell Biol. 2005;7(10):1014-1020.

31. Zhao M, Quan Y, Zeng J, Lyu X, Wang H, Lei JH, et al. Cullin3 deficiency shapes tumor microenvironment and promotes cholangiocarcinoma in liver-specific Smad4/Pten mutant mice. Int J Biol Sci. 2021;17(15):4176-4191.

32. Morandell J, Schwarz LA, Basilico B, Tasciyan S, Dimchev G, Nicolas A, et al. *Cul3* regulates cytoskeleton protein homeostasis and cell migration during a critical window of brain development. Nat Commun. 2021;12(1):3058.

33. Maeoka Y, Cornelius RJ, Ferdaus MZ, Sharma A, Nguyen LT, McCormick JA. Cullin 3 mutant causing familial hyperkalemic hypertension lacks normal activity in the kidney. Am J Physiol Renal Physiol. 2022;323(5):F564-F576.

34. Li X, Yang KB, Chen W, Mai J, Wu XQ, Sun T, et al. *CUL3* (cullin 3)-mediated ubiquitination and degradation of BECN1 (beclin 1) inhibit autophagy and promote tumor progression. Autophagy. 2021;17(12): 4323-4340.

35. Wu Y, Zhao M, Lin Z. Pyrroloquinoline quinone (PQQ) alleviated sepsis-induced acute liver injury, inflammation, oxidative stress and cell apoptosis by downregulating *CUL3* expression. Bioengineered. 2021;12(1):2459-2468.

36. Ji X, Yang X, Gu X, Chu L, Sun S, Sun J, et al. *CUL3* induces mitochondrial dysfunction *via* MRPL12 ubiquitination in renal tubular epithelial cells. FEBS J. 2023;290(22):5340-5352.

37. Huotari J, Meyer-Schaller N, Hubner M, Stauffer S, Katheder N, Horvath P, et al. Cullin-3 regulates late endosome maturation. Proc Natl Acad Sci USA. 2012;109(3):823-828.

38. Chen S, Novick P, Ferro-Novick S. ER structure and function. Curr Opin Cell Biol. 2013;25(4):428-433.

39. Phillips MJ, Voeltz GK. Structure and function of ER membrane contact sites with other organelles. Nat Rev Mol Cell Biol. 2016;17(2):69-82.

40. Friedman JR, Voeltz GK. The ER in 3D: A multifunctional dynamic membrane network. Trends Cell Biol. 2011;21(12):709-717.

41. Yuniati L, Lauriola A, Gerritsen M, Abreu S, Ni E, Tesoriero C, et al. Ubiquitylation of the ER-shaping protein Lunapark *via* the CRL3(KLHL12) ubiquitin ligase complex. Cell Rep. 2020;31(7):107664.

42. Zhao Y, Sun Y. Cullin-RING Ligases as attractive anti-cancer targets. Curr Pharm Des. 2013;19(18):3215-3225.

43. Jerabkova K, Sumara I. Cullin 3, a cellular scripter of the non-proteolytic ubiquitin code. Semin Cell Dev Biol. 2019;93:100-110.